04

Study of the process of holographic formation of multiplexed chirped multilayer diffraction structures formed in a photopolymer material with liquid crystals

© S.N. Sharangovich, V.O. Dolgirev, D.S. Rastrygin

Tomsk State University of Control Systems and Radioelectronics, Tomsk, Russia

e-mail: shr@tusur.ru

Received December 28, 2024
Revised February 27, 2025
Accepted March 01, 2025

A generalized analytical model is presented that takes into account the temporary change in the initial conditions of holographic formation due to the photoinduced change in the optical absorption of multiplexed chirped multilayer inhomogeneous holographic diffraction structures formed in a photopolymer material with a high proportion of nematic liquid crystals. Using numerical simulation, it was shown that during the formation of each individual diffraction grating in each individual layer, the refractive index profile can have a two-dimensional inhomogeneity, which is caused by both the photoinduced absorption of the material and the phase inhomogeneity of the recording radiation. Thus, the developed analytical model allows one to determine in advance the type of grating profile for chirped multilayer holographic diffraction structures, which is necessary for a more accurate determination of the diffraction characteristics of such structures.

Keywords: photopolymer materials, liquid crystals, multilayer diffraction structures.

DOI: 10.61011/EOS.2025.04.61411.7513-24

Introduction

Over the past fifteen years, the application of emerging liquid crystal (LC) materials technologies has led to significant engineering and scientific advances in photonics [1]. Micro- and nanotechnologies, which enabled significant progress in the production of tunable photonic devices based on LC materials, have become particularly important. These devices include optical switches, tunable attenuators, photonic crystal fibers, optical filters, diffraction gratings, vortex phase plates, lasers, etc. [2–8].

Multilayer inhomogeneous holographic diffractive structures (MIHDSs) are presently attracting more and more research attention. Their characteristic feature is the presence of interference effects between diffraction layers that are separated by buffer layers. The selective response of diffracted radiation of such structures is a set of local maxima that depends on the number and thickness ratio of the buffer and diffraction layers [9]. These diffracting elements have various potential applications in photonics; e.g., they may be used to construct optical spectral filters or generate femtosecond laser pulses.

Although such multilayer structures have been examined in numerous studies, their further improvement (e.g., broadening the angular and spectral characteristics, which would help increase the overall bandwidth) remains a relevant objective.

One of the possible ways toward this goal is the use of an integrated approach to the formation of multiplexed MIHDSs with a variable period. First, sequential recording (multiplexing) of several gratings provides an opportunity to broaden both the angular and spectral characteristics by combining the angular selectivities of recorded photonic structures. Notably, this broadening may be almost a multiple of the number of recorded gratings. Second, chirped structures, which are characterized by variation of the period along the grating vector, may be formed in the process of recording of holographic diffraction structures by optical radiation with an inhomogeneous phase front. Owing to this period variation, such structures also undergo broadening of the angular and, accordingly, spectral characteristics [10,11]. Having combined multiplexing and chirping, one may achieve manyfold broadening of the angular and spectral characteristics of conventional MIHDSs [10–17].

Another important task is to find a way to control the diffraction characteristics of such structures. One solution is to use a photosensitive medium with embedded liquid crystals (e.g., thin films with a light-sensitive photopolymer material (PPM) and nematic LCs) for holographic recording. As was demonstrated in [18], an external electric field acting on a diffraction layer with PPM-LC allows one to control both the level of diffraction efficiency and the shift in angular selectivity. Thus, the present study is focused on the use of a PPM-LC light-sensitive medium, which should enable control over diffraction characteristics through the application of an electric field, for holographic recording of chirped MIHDSs.

The aim of the study is to develop a generalized analytical model sensitive to the temporary change in the initial conditions of holographic formation as a result of the photoinduced variation of optical absorption (PIA) of multiplexed chirped MIHDSs in PPM-LC and to investigate

the process of their formation in linear and nonlinear recording modes.

Theoretical model of formation of multiplexed chirped MIHDSs in PPM-LC

Multiplexed chirped MIHDSs are formed by two plane monochromatic light waves with different phase distributions. One wave has a homogeneous phase distribution E_0, while the other has an inhomogeneous distribution E_1. Light beams are incident at angles θ_0 and θ_1 onto a complex multilayer PPM-LC structure (Fig. 1).

Each layer of this structure is an anisotropic medium, which entails splitting of a light beam inside the material into two waves (ordinary and extraordinary) [17]. When a monochromatic wave passes through a diffraction layer, the initial conditions change due to attenuation caused by photoinduced absorption [18]. The intensity of the light field interference pattern in the region of interaction of two recording light beams is [19]

$$I^{i,n,m}(t,\mathbf{r}) = \sum_{m=o,e} I^{i,n,m}_{sum}(t,\mathbf{r})\left[1 + m^{i,n,m}(t,\mathbf{r})\cos(\varphi^{i,n}(\mathbf{r}))\right], \tag{1}$$

where $\varphi^{i,n}(\mathbf{r}) = \varphi^{i,n}_0 + \nabla\varphi^{i,n}\mathbf{r} + 0.5\varphi^{i,n}\mathbf{r}^2$; $|\nabla\varphi^{i,n}| = \varphi^{i,n,'} = K^{i,n}_1$ — average magnitude of vector $\mathbf{K}^{i,n}_1$; $0.5\varphi^{i,n} = \varphi^{i,n,'}$ — shift of the magnitude of grating vector $\mathbf{K}^{i,n}_1$ relative to the average value; $m^{i,n,m}(t,\mathbf{r}) = 2\sqrt{I^{i,n,m}_0(t,\mathbf{r})I^{i,n,m}_1(t,\mathbf{r})}(\mathbf{e}_0\mathbf{e}_1)/\left(I^{i,n,m}_0(t,\mathbf{r}) + I^{i,n,m}_1(t,\mathbf{r})\right)$ — local interference pattern contrast; i — number of the recorded holographic diffraction structure (HDS); $I^{i,n,m}_{sum}(t,\mathbf{r}) = \left[I^{i,n,m}_0(t,\mathbf{r}) + I^{i,n,m}_1(t,\mathbf{r})\right]$; $I^{i,n,m}_0(t,\mathbf{r}) = I^{i,0,n,m}(t,\mathbf{r})\cdot e^{-\alpha^{i,n,m}(t,\mathbf{r})y/\cos(\theta^{i,m}_0)}$; $I^{i,n,m}_1(t,\mathbf{r}) = I^{i,1,n,m}(t,\mathbf{r})\cdot e^{-\alpha^{i,n}(t,\mathbf{r})y/\cos(\theta^{i,m}_1)}$; $I^{i,j,n,m}(\mathbf{r}) = |E^{i,n,m}_j(\mathbf{r})|^2$; $j = 0, 1$; $m = o, e$; $\mathbf{K}^{i,n,m}_1 = \mathbf{k}^{i,n,m}_0 - \mathbf{k}^{i,n,m}_1$ — grating vector; $\mathbf{r}$ — radius vector; $\mathbf{k}^{i,n,m}_j$ — wave vectors of beams; $\alpha^{i,n,m}(t,\mathbf{r}) = \alpha^{i,n}_2 + \alpha^{i,n}_1\exp\left[-\left(I^{i,n,m}_0(t,\mathbf{r})/\cos(\theta^i_0) + I^{i,n,m}_1(t,\mathbf{r})/\cos(\theta^i_1)\right)y\,t/T^{i,n}_a\right]$ — PIA coefficient; $n = 1, 2, \ldots, N$ — layer number; $\alpha^{i,n}_1 = \alpha_0 K^{i,n}_0$ and α_2 — absorption components for the dye and the substrate (in the present case, the substrate is a protective film, which acts a buffer layer, on both sides of the PPM, and the dye, which is a much better absorber than the substrate, is needed to absorb light of a certain wavelength, which causes its excitation and interaction with the initiator and results in the formation of primary radicals; after that, it passes into an inactive colorless state (leuco form), having fulfilled its part in initiation of chemical processes); α_0 — absorption component of the dye molecule; ϕ — quantum efficiency of the dye; and $T^{i,n}_a = 1/\left(\phi\alpha_0\max[I^{i,n}_0(t,\mathbf{r})]\right)$.

The notation in Fig. 1 is as follows: $E_0(\mathbf{r},t)$, $E_1(\mathbf{r},t)$ are the homogeneous and inhomogeneous monochromatic light waves; θ^i_0, θ^i_1 are the angles of incidence of waves onto the sample; ψ is the sample rotation angle; $\mathbf{k}^{i,e}_0, \mathbf{k}^{i,e}_1$ are the wave vectors of homogeneous and inhomogeneous monochromatic light waves; $\theta^{i,0}_0, \theta^{i,e}_1$ are the angles of propagation of wave vectors; d is the diffraction layer thickness, and t is the buffer layer thickness.

The kinetic equations of monomer concentration and refraction index characterize the formation of each PPM-LC layer in the multiplexed MIHDS. However, a spatially inhomogeneous function $M^{i,n,m}(t,\mathbf{r})$ of the monomer concentration variation rate induces a concentration gradient and diffusion in better illuminated regions.

It is important to bear in mind that the monomer concentration gradient does not only affect the process of formation of each PPM-LC layer, but also influences its properties. Thus, control of the monomer concentration gradient may be an important factor in the production of multiplexed chirped MIHDSs.

The monomer concentration in chemical reactions proceeding in exposed photopolymerizing materials may change for various reasons. However, one may formulate an equation for monomer concentration variation rate $M^{i,n,m}(t,\mathbf{r})$ by combining both factors causing these changes:

$$\partial M^{i,n,m}(t,\mathbf{r})/\partial t = \mathrm{div}\left(D^{i,n,m}_M(t,\mathbf{r})\mathrm{grad}(M^{i,n,m}(t,\mathbf{r}))\right) - h[I^{i,n,m}(t,\mathbf{r})]^k M^{i,n,m}(t,\mathbf{r}), \tag{2}$$

where $D^{i,n,m}_M(t,\mathbf{r})$ is the monomer diffusion coefficient and h is a parameter characterizing the interaction of radiation with the monomer.

Another factor worthy of note in the description of diffusion processes is diffusion coefficient change $D^{i,n,m}_M(t,\mathbf{r})$ in the course of HDS formation:

$$D^{i,n,m}_M(t,\mathbf{r}) = D^{i,n}_{00}\exp\left[-s(1 - M^{i,n,m}(t,\mathbf{r})/M^{i,n}_{00})\right], \tag{3}$$

where $M^{i,n}_{00}$ and $D^{i,n}_{00}$ define the initial concentration and diffusion coefficient of the monomer, respectively, and parameter s characterizes the diffusion variation rate.

Photopolymerization occurring in the process of holographic formation induces a change in the monomer concentration and, consequently, the density of polymer molecules. The equation characterizing the change in polymer concentration may be written as follows:

$$\partial P^{i,n,m}(t,\mathbf{r})/\partial t = F^{i,n,m}(t,\mathbf{r})\,M^{i,n,m}(t,\mathbf{r}), \tag{4}$$

where $F^{i,n,m}(t,\mathbf{r}) = k^{i,n}_R I^{i,n,m}(t,\mathbf{r})$ is a function of polymerization rate, which depends on polymerization proportionality coefficient $k^{i,n}_R$ and recording field intensity $I^{i,n,m}(t,\mathbf{r})$.

The process of formation is associated with complex processes at the molecular level that involve LC molecules. However, their contribution is limited to the diffusion process. It should be borne in mind that the rate of change of the LC concentration in the material is of significant importance for determining the material properties and quality. Therefore, the equation characterizing this process takes the form

$$\partial L^{i,n,m}(t,\mathbf{r})/\partial t = \mathrm{div}\left(D^{i,n,m}_{LC}(t,\mathbf{r})\mathrm{grad}(L^{i,n,m}(t,\mathbf{r}))\right), \tag{5}$$

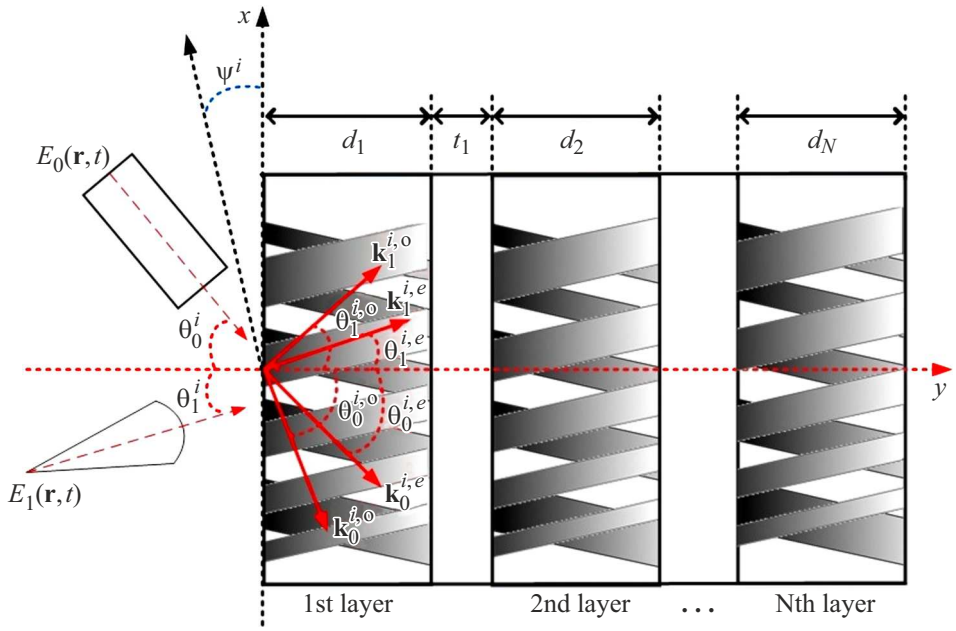

Figure 1. Diagram of recording of multiplexed chirped MIHDSs in PPM-LC.

where function $D_{LC}^{i,n,m}(t, \mathbf{r})$ defines the diffusion coefficient of LC molecules.

Since the process of diffraction layer formation is complex and multi-staged and involves various physical and chemical processes, it is necessary to examine in more detail the influence of the number of monomer and LC molecules on the obtained result.

It is important to note that the constancy of the number of monomer and LC molecules is a key factor in the formation of the diffraction layer. If this condition is violated, the equilibrium of the system shifts; in addition, one needs to take into account that the medium in which the diffraction layer is formed is two-component. This implies that the monomer and LC molecules interact with each other via diffusion, which may have a significant influence on the resulting characteristics of the diffraction structure. In accordance with Fick's first law, the vector densities for the monomer ($\mathbf{J}_M^{i,n,m}$) and LCs ($\mathbf{J}_{LC}^{i,n,m}$) are equal in magnitude, but the vector directions are opposite:

$$\mathbf{J}_M^{i,n,m} = -\mathbf{J}_{LC}^{i,n,m}.$$

A change in the LC concentration also affects the characteristics of the system. The equation used to characterize this process may be written in terms of the monomer concentration variation:

$$\partial L^{i,n,m}(t, \mathbf{r})/\partial t = -\mathrm{div}\left(D_{LC}^{i,n,m}(t, \mathbf{r})\mathrm{grad}(M^{i,n,m}(t, \mathbf{r}))\right). \quad (6)$$

Local variations of density of the PPM-LC layers induced by changes in the concentration of all three components lead to a change in refraction index $n^{i,n,m}(t, \mathbf{r})$. The Lorentz–Lorenz formula may be used to characterize this change:

$$\frac{\partial n^{i,n,m}(t, \mathbf{r})}{\partial t} = \frac{4\pi}{3}\frac{((n_{st}^i)^2+2)^2}{6(n_{st}^i)^2}\left(\alpha_M^{i,n}\frac{\partial M^{i,n,m}(t, \mathbf{r})}{\partial t} + \alpha_p^{i,n}\frac{\partial P^{i,n,m}(t, \mathbf{r})}{\partial t} + \alpha_{LC}^{i,n}\frac{\partial L^{i,n,m}(t, \mathbf{r})}{\partial t}\right), \quad (7)$$

where $\alpha_M^{i,n}, \alpha_p^{i,n}$ and $\alpha_{LC}^{i,n}$ define the polarizability of monomer, polymer, and LC molecules, respectively, and n_{st}^i defines the initial refraction index value prior to recording of the ith HDS.

It follows from the above Eqs. (2) and (7) that the change in refraction index during photopolymerization depends on the number of particles, which remains constant:

$$M^{i,n,m} + l \cdot P^{i,n,m} = \mathrm{const},$$

where l is the average polymer chain length. The refraction index of the polymer component varies in time and is written as

$$\partial n^{i,n,m}(t, \mathbf{r})/\partial t|_p = \delta n_p^{i,n}(\partial M^{i,n,m}(t, \mathbf{r})/\partial t), \quad (8)$$

where parameter

$$\delta n_p^{i,n} = \frac{4\pi}{3}\frac{((n_{st}^i)^2+2)^2}{6(n_{st}^i)^2}\left(\alpha_M^{i,n} + \frac{\alpha_P^{i,n}}{l}\right)\frac{M_M^{i,n}}{W_M^{i,n}}$$

specifies the change in refraction index caused by polymerization of the monomer, and elements $M_M^{i,n}$ and $W_M^{i,n}$ characterize the density and molecular weight of monomer molecules.

Equations (2), (6), and (7) allow one to formulate an expression for the refraction index variation caused by the

displacement of LC molecules by the monomer into the dark region:

$$\partial n^{i,n,m}(t,\mathbf{r})/\partial t|_d = -\delta n_d^{i,n}\mathrm{div}\big(D_{LC}^{i,n,m}(t,\mathbf{r})\mathrm{grad}(M^{i,n,m}(t,\mathbf{r}))\big), \quad (9)$$

where parameter

$$\delta n_d^{i,n} = \frac{4\pi}{3}\frac{((n_{st}^i)^2+2)^2}{6(n_{st}^i)^2}\left(\alpha_M^{i,n}\frac{M_M^{i,n}}{W_M^{i,n}} + \alpha_{LC}^{i,n}\frac{L_{LC}^{i,n}}{W_{LC}^{i,n}}\right)$$

specifies the change in refraction index caused by interdiffusion of the monomer and LC molecular components, and $W_{LC}^{i,n}$ and $L_{LC}^{i,n}$ characterize the molecular weight and density of LC molecules.

The expression for refraction index variation incorporating both photopolymerization and diffusion recording mechanisms is as follows:

$$\partial n^{i,n,m}(t,\mathbf{r})/\partial t = \partial n^{i,n,m}(t,\mathbf{r})/\partial t|_p + \partial n^{I,n,m}(t,\mathbf{r})/\partial t|_d.$$

Equations (2), (8), and (9), which depend on just one component (monomer concentration), are a replacement for Eq. (7), which depended on three components. However, despite this simplification, the solutions to these equations still remain nonlinear. In order to solve them, one should use a Fourier series expansion in spatial harmonics of gratings with account for the monomer concentration and the refraction index:

$$\begin{cases} M^{n,m}(t,\mathbf{r}) = \\ \sum\limits_{i=1}^{N_s}\Big[M_0^{i,n,m}(t,\mathbf{r}) + \sum\limits_{j=1}^{N} M_j^{i,n,m}(t,\mathbf{r})\cos(j\mathbf{K}^{i,n,m}\mathbf{r})\Big], \\ \Delta n_p^{n,m}(t,\mathbf{r}) = \\ \sum\limits_{i=1}^{N_s}\Big[\Delta n_{0,p}^{i,n,m}(t,\mathbf{r}) + \sum\limits_{j=1}^{N} \Delta n_{j,p}^{i,n,m}(t,\mathbf{r})\cos(j\mathbf{K}^{i,n,m}\mathbf{r})\Big], \\ \Delta n_{LC}^{n,m}(t,\mathbf{r}) = \\ \sum\limits_{i=1}^{N_s}\Big[\Delta n_{0,LC}^{i,n,m}(t,\mathbf{r}) + \sum\limits_{j=1}^{N} \Delta n_{j,LC}^{i,n,m}(t,\mathbf{r})\cos(j\mathbf{K}^{i,n,m}\mathbf{r})\Big], \end{cases} \quad (10)$$

where $M_j^{i,n,m}$, $\Delta n_{j,p}^{i,n,m}$, and $\Delta n_{j,LC}^{i,n,m}$ are the Fourier coefficients of the function for harmonics of the monomer, polymer, and LC component concentration and N_s is the number of multiplexed HDSs.

The solutions obtained from Eqs. (10) are used for a spatially inhomogeneous refraction index distribution in a medium. They are determined by finding the sum relative to the zero and first harmonics of the monomer concentration and refraction index, which are obtained from kinetic equations (2), (8), and (9). Let us introduce the corresponding initial conditions that will allow us to obtain the sought-for solutions:

$$\begin{cases} M_0^{i,n}(t=0,\mathbf{r}) = M_{00}^n - \sum\limits_{g=0}^{i-1} M_0^{g,n}, \\ \Delta n_{0,p}^{i,n}(t=0,\mathbf{r}) = 0; \Delta n_{0,LC}^{i,n}(t=0,\mathbf{r}) = n_{LC}^{i,n}, \\ M_0^{i,n}(t=0,\mathbf{r}) = 0, \Delta n_{1,p}^{i,n}(t=0,\mathbf{r}) = 0; \\ \Delta n_{1,LC}^{i,n}(t=0,\mathbf{r}) = 0. \end{cases}$$

Taking into account the properties of orthogonality of harmonics and inserting (10) into expressions (2), (8), and (9), one may write the equations for the first harmonic of the monomer concentration and refraction index induced by two recording mechanisms (photopolymerization and diffusion):

$$\begin{cases} \frac{\partial M_1^{i,n,m}}{\partial t} = -\exp(-s[1-M_0^{i,n}/M_0^{i,n}(t=0)])M_1^{i,n} - \\ \frac{2^k}{b^{i,n,m}}km^{i,n,m}M_0^{i,n} - M_1^{i,n}\frac{2^k}{b^{i,n,m}}\Big[1+\frac{3}{8}k(k-1)m^{i,n,m}\Big], \\ \frac{\partial \Delta n_{1,LC}^{i,n,m}}{\partial t} = -\delta n_d^{i,n}\frac{D^{i,n}}{L}\exp\Big(-s\Big(1-\frac{M_0^{i,n}}{M_{00}^{i,n}}\Big)\Big)M_1^{i,n}, \\ \frac{\partial \Delta n_{1,p}^{i,n,m}}{\partial t} = \delta n_p^{i,n}\frac{2^k}{b^{i,n,m}}\Big[k\frac{M_0^{i,n}}{M_{00}^{i,n}} + \Big(1+\frac{3}{8}k(k-1)m^{i,n,m}\Big)\frac{M_1^{i,n}}{M_{00}^{i,n}}\Big], \end{cases} \quad (11)$$

where parameter $b^{i,n,m}$ specifies the recording conditions at each moment in time and at each point of the PPM-LC layer and is characterized by the ratio of diffusion and polymerization times.

Integrating for $\Delta n_{1LC}^{i,n,m}$ and $\Delta n_{1p}^{i,n,m}$ from (11), we obtain the final expression for the spatial distribution of amplitude of the first harmonic of the refraction index, which is a sum of contributions of the photopolymer and LC components:

$$n_1^{i,n,m}(t,y,x) = n_{1p}^{i,n,m}(t,y,x) + n_{1LC}^{i,n,m}(t,y,x), \quad (12)$$

where

$$n_{1p}^{i,n,m}(t,y,x) = \delta n_p\frac{2^k}{b^{i,n,m}(t,y,x)}\int\limits_{\tau_f^i}^{t} I_{0n}^{i,n,m}(\tau,y,x)\Big[p^{i,n,m}(t,y,x)$$

$$km^{i,n,m}(t,y,x) - f^{i,n,m}(t,y,x)\big(1+1.5L^{i,n,m}(\tau,y,x)\big)\Big]d\tau$$

and

$$n_{1LC}^{i,n,m}(t,y,x) = \delta n_{LC}\frac{D_{LC}}{D_m}\int\limits_{\tau_f^i}^{t} f^{i,n,m}(\tau,y,x)b^{i,n,m}(\tau,y,x)d\tau$$

— amplitude profiles of the polymer and LC gratings; δn_{LC} and δn_m — coefficients of refraction index variation of LCs and the polymer; D_{LC} and D_m — diffusion coefficients of LCs and the monomer;

$$b^{i,n,m}(t,y,x) = \frac{T_p^{i,n,m}(t,y,x)}{T_m^{i,n,m}(t,y,x)}\Big(1+\frac{\varphi^{i,''}\cdot x}{\varphi^{i,'}}\Big)^2;$$

polymerization time —

$$T_p^{i,n,m}(t,y,x) = 1/\big(K_g K_b^{-k}(\alpha_0\beta\langle K^{i,n}\rangle I^{i,n,m}(t,y,x)\tau_0)^k\big);$$

$$T_m^{i,n,m}(t,y,x) = \big[D_m|\varphi^{i,'}|^2\big]^{-1}$$

— diffusion time, $\langle K^{i,n}\rangle$ — dye concentration; K_g and K_b determine the values of growth and termination coefficients of the polymer chain; parameter β characterizes the photoinitiation reaction; parameter τ_0 sets the lifetime in the excited state;

$$p^{i,n,m}(y,y,x) = \exp\Big[\frac{-2^k}{b^{i,n,m}(t,y,x)}(1+L^{i,n,m}(t,y,x))t\Big];$$

$$L^{i,n,m}(t,y,x) = k(k-1)\frac{[m^{i,n,m}(t,y,x)]^2}{4};$$

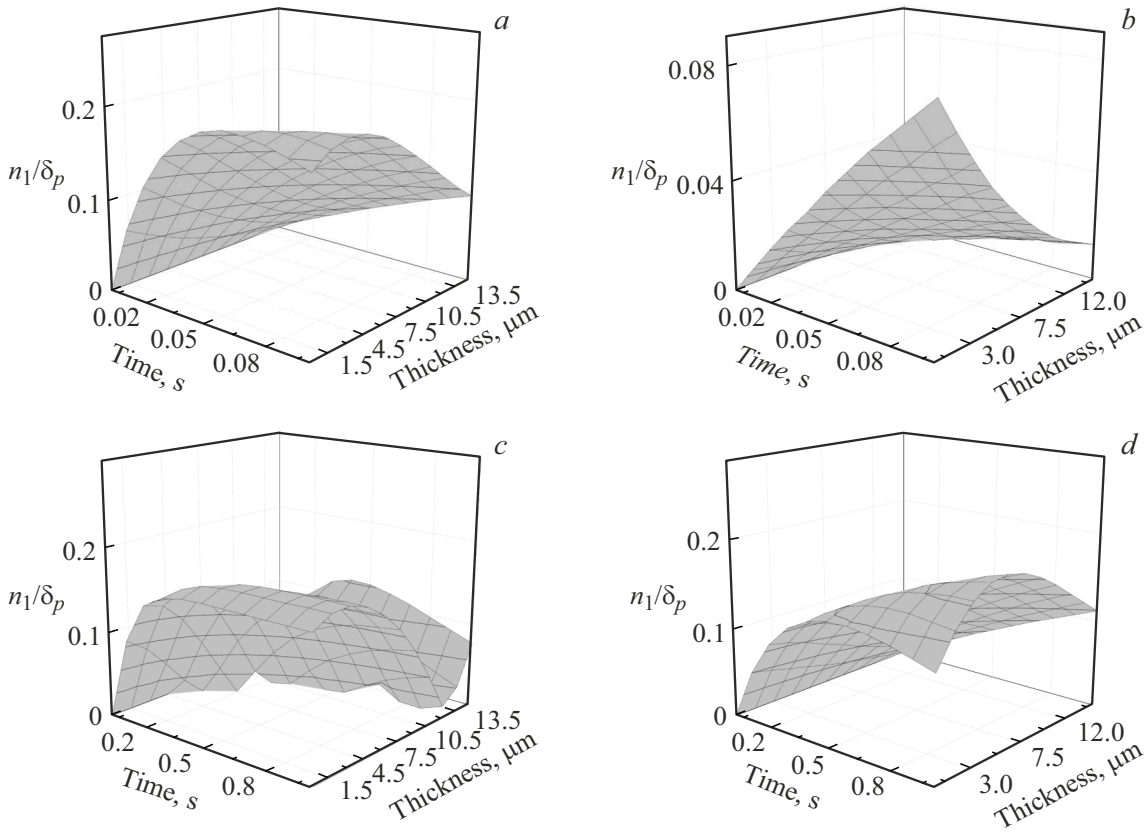

Figure 2. Kinetics of spatial profiles of the first harmonic of the refraction index of a two-layer multiplexed chirped MIHDS in the nonlinear recording mode for two gratings on the first *(a, b)* and second layers *(c, d)*.

k — parameter of the degree of nonlinearity of the process; $b_m^{i,n,m}(t,y,x) = (1+\varphi^{i,'}x/\varphi^{i,'})^2 \exp\left[-s(1-p^{i,n,m}(t,y,x))\right]$; s — parameter of the diffusion variation rate; $I_{0n}^{i,n,m}(t,y,x) = I_{sum}^{i,n,m}(t,y,x)/\max[I_{sum}^{i,n,m}(t,y,x)]$ — normalized beam intensity in the nth layer, $f^{i,n,m}(t,y,x) = \frac{2^k}{b^{i,n,m}(t,y,x)} k \int\limits_{\tau_f^i}^{t} p^{i,n,m}(\tau,y,x) m^{i,n,m}(\tau,y,x) \times I_{on}^{i,n,m}(\tau,y,x) \exp\left[-1 \int\limits_{\tau}^{t} b_m^{i,n,m}(T,y,x) + \frac{2^k}{b^{i,n,m}(T,y,x)} \times I_{0n}^{i,n,m}(T,y,x)\left(1+1.5L^{i,n,m}(T,y,x)\right) dT\right] d\tau$, τ_f^i — end time of the previous HDS recording.

The generalized analytical model presented in this section characterizes the process of formation of multiplexed electrically controlled multilayer inhomogeneous holographic diffraction structures with a variable period in photopolymerizing compositions containing nematic liquid crystals. The conditions of photoinduced optical absorption were discussed, and an expression allowing one to determine the kinetics of formation of the spatiotemporal distribution of amplitude of the first harmonic of the refraction index for each diffraction layer in each recorded photonic structure was formulated.

Thus, the developed analytical model provides an opportunity to specify in advance the type of grating profile for multiplexed chirped multilayer holographic diffraction structures, which is needed for more accurate determination of diffraction characteristics of the structures under study.

Numerical modeling

The process of forming a two-layer multiplexed chirped MIHDS with PPM-LC, which has two diffraction structures recorded sequentially at an angle in each PPM-LC layer, was studied via numerical simulation based on the presented model and the obtained analytical solutions. The values of PPM parameters corresponded to those of the materials studied at the Vorozhtsov Novosibirsk Institute of Organic Chemistry (Siberian Branch, Russian Academy of Sciences) and the photopolymer materials produced by Geola [20,21]: $\lambda = 633\,\text{nm}$ — recording wavelength; $d_n = 15\,\mu\text{m}$ — diffraction layer thickness; $\alpha_2 = 0.015\,\text{Np}$ — substrate (film protecting the PPM) absorption coefficient, $\alpha_1 = 1.92\,\text{Np}$ — absorption coefficient of the material (the photopolymer layer itself), $k = 0.5$ — parameter of the degree of nonlinearity of the recording process, $s = 1$ — diffusion variation rate parameter, $2\theta = 30^\circ$ — angle between the recording beams, $\delta_{np} = 0.09$ — coefficient of variation of the polymer refraction index, $\delta_{ni} - 0.1\delta_{np}$ — coefficient of variation of

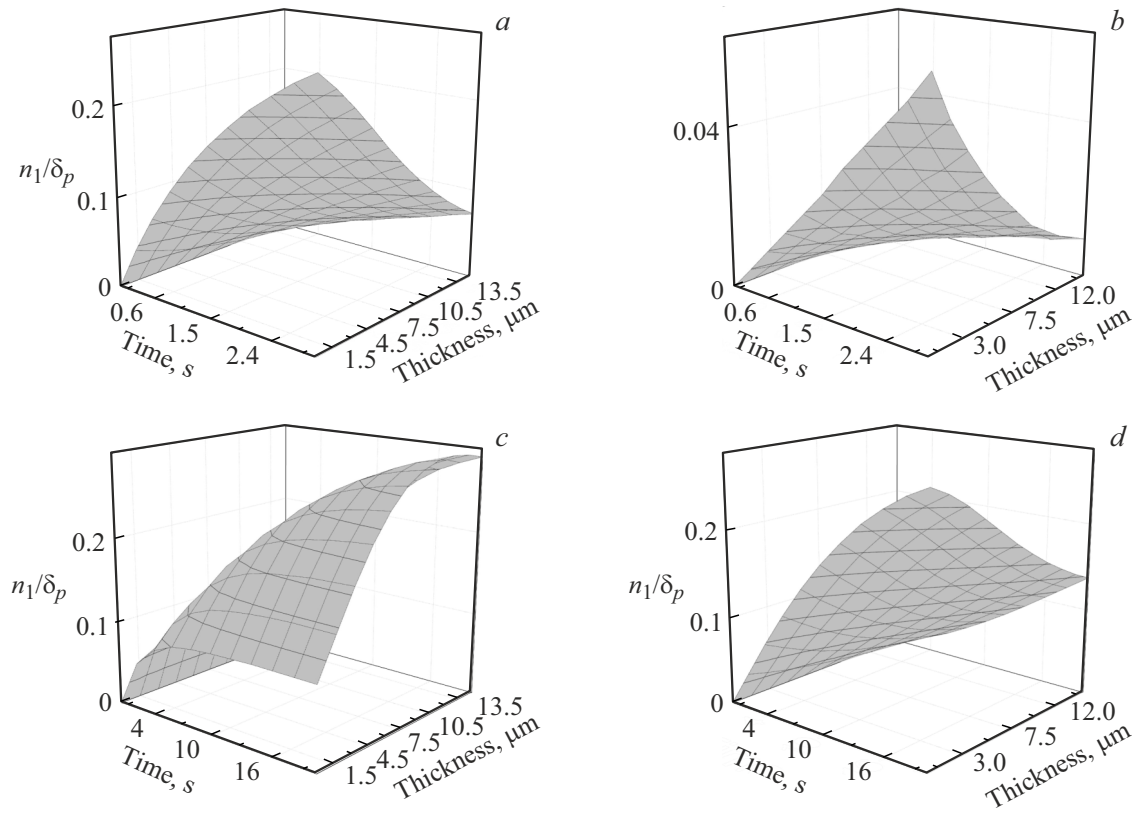

Figure 3. Kinetics of spatial profiles of the first harmonic of the refraction index of a two-layer multiplexed chirped MIHDS in the linear recording mode for two gratings on the first *(a, b)* and second layers *(c, d)*.

the LC refraction index, $D_m = 15 \cdot 10^{-12}\,\mathrm{m^2/s}$ — monomer diffusion coefficient, $D_{LC} = D_m$ — LC diffusion coefficient, δ_p — coefficient of variation of the refraction index, and $0.5\nabla^2\varphi = 3 \cdot 10^9\,\mathrm{mm^{-1}}$ — deviation of the **K** vector magnitude from the average value. The influence of deviation of the vector magnitude on the selective response was discussed in [11].

Figure 2 shows the kinetics of spatial profiles of the first harmonic of the refraction index of a two-layer multiplexed chirped MIHDS as functions of the recording time and the PPM-LC layer thickness in the nonlinear recording mode ($b = 0.1$) for two gratings on the first (Figs. 2, *a, b*) and second layers (Figs. 2, *c, d*), respectively.

It can be seen from Fig. 2 that unique spatial profiles correspond to each layer and each grating. While the depth for the first grating decreases from one layer to the other, the profile of the second grating is transformed in width and depth. This is attributable to the nonlinear recording mode, wherein the monomer does not have enough time to diffuse into light areas and polymerizes quickly, and to the PIA process itself: the material is bleached in the course of recording, which also induces changes in the recording conditions.

Figure 3 shows the kinetics of spatial profiles of the first harmonic of the refraction index of a two-layer multiplexed chirped MIHDS as functions of the recording time and the PPM-LC layer thickness in the linear recording mode ($b = 5$) for two gratings on the first (Figs. 3, *a, b*) and second layers (Figs. 3, *c, d*).

It is evident from Figs. 3, *a, b* that the depth of the refraction index profile for the first layer of the first grating decreases in the process of recording; in the case of the second grating, the depth increases. This is attributable to the fact that during recording, the monomer first diffuses rapidly into the light region at the nearest point of the layer for the first grating; as for the second grating, the remaining monomer at the end of the layer also starts polymerizing rapidly, but due to bleaching of the material. The polymerization process for the second layer of the first grating is delayed due to the low intensity of the recording light beams, which is caused by photoinduced absorption. At the same time, the polymerization process for the second grating is, in contrast, intensified, since the material was bleached during the formation of the first grating. It is also worth noting that the profile for the second layer has the same character of depth reduction, which is attributable to a more homogeneous diffusion of the monomer into lighter areas due to delayed bleaching of the material (relative to the first layer). In contrast to the nonlinear mode, the amplitude for the first layer increases by 50% when the linear recording mode is used.

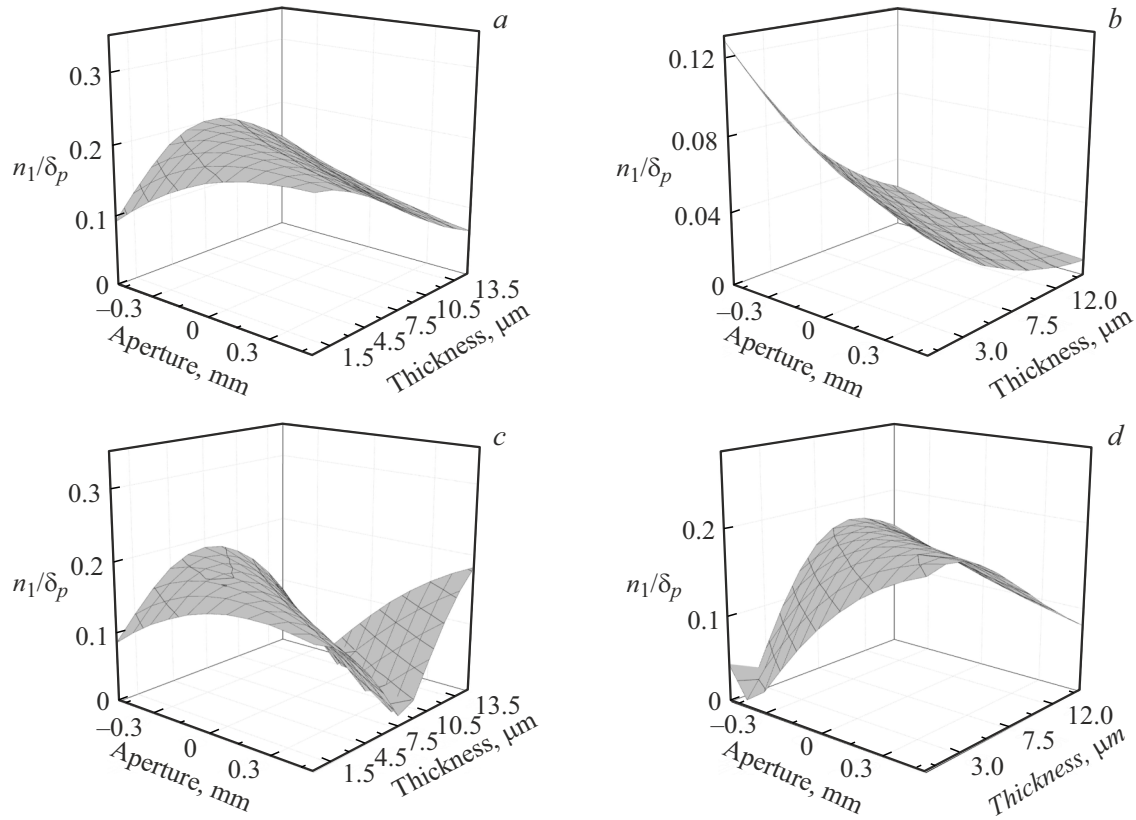

Figure 4. Two-dimensional spatial profiles of the first harmonic of the refraction index in the nonlinear recording mode for two gratings on the first (a, b) and second layers (c, d).

Figure 4 shows the formed spatial profiles of the first harmonic of the refraction index of a two-layer multiplexed chirped MIHDS as functions of the PPM-LC layer width and thickness in the nonlinear recording mode $(b = 0.1)$ for two gratings on the first (Figs. 4, *a, b*) and second layers (Figs. 4, *c, d*), respectively.

It can be seen from Fig. 4 that the refraction index profiles for each layer and each grating in the nonlinear recording mode have a pronounced two-dimensional inhomogeneity over depth and thickness of the PPM-LC layer. The inhomogeneity over layer width is caused in this case by the influence of phase inhomogeneity of recording radiation, which induces variation of the structure period over sample width. Depending on the chosen recording time for each grating (in the present case, $t = 0.1$ s for the first grating and $t = 1$ s for the second one), the refraction index profile in the nonlinear recording mode may also undergo a significant transformation, which is illustrated clearly by Figs. 4, *b, d* that present the profile for the second grating of the first layer.

Figure 5 shows the recorded spatial profiles of the first harmonic of the refraction index of a two-layer multiplexed chirped MIHDS as functions of the PPM-LC layer width and thickness in the linear recording mode $(b = 5)$ for two gratings on the first (Figs. 5, *a, b*) and second layers (Figs. 5, *c, d*), respectively.

It follows from Fig. 5 that the refraction index profiles also have two-dimensional inhomogeneity over layer thickness and depth in the linear recording mode. However, the nature of variation over layer thickness for the second grating differs from the one observed in the nonlinear recording mode; this is attributable to faster diffusion of the monomer into bleached areas and bleaching of the material itself. It is also worth noting that the profile for the second grating on the first layer has a dome shape; its amplitude increases by 65% within the thickness range from 0 to 14 μm and decreases by 5% at 14–20 μm, but maintains a constant nature within the aperture range from minus 0.5 to 0.5 mm. In contrast, the profile on the second layer is decreasing over thickness and aperture. The increase in amplitude of the spatial profile for the first layer (by an average of 62.5%) relative to the nonlinear recording mode is also worthy of note.

It was demonstrated through numerical modeling that the refraction index profile may have a pronounced two-dimensional inhomogeneity during the formation of each individual diffraction grating in each individual layer, which is attributable both to photoinduced absorption of the material and to phase inhomogeneity of recording radiation.

Thus, the formation of multiplexed chirped MIHDSs in the nonlinear recording mode may exert a negative influence on diffraction characteristics due to the enhancement of

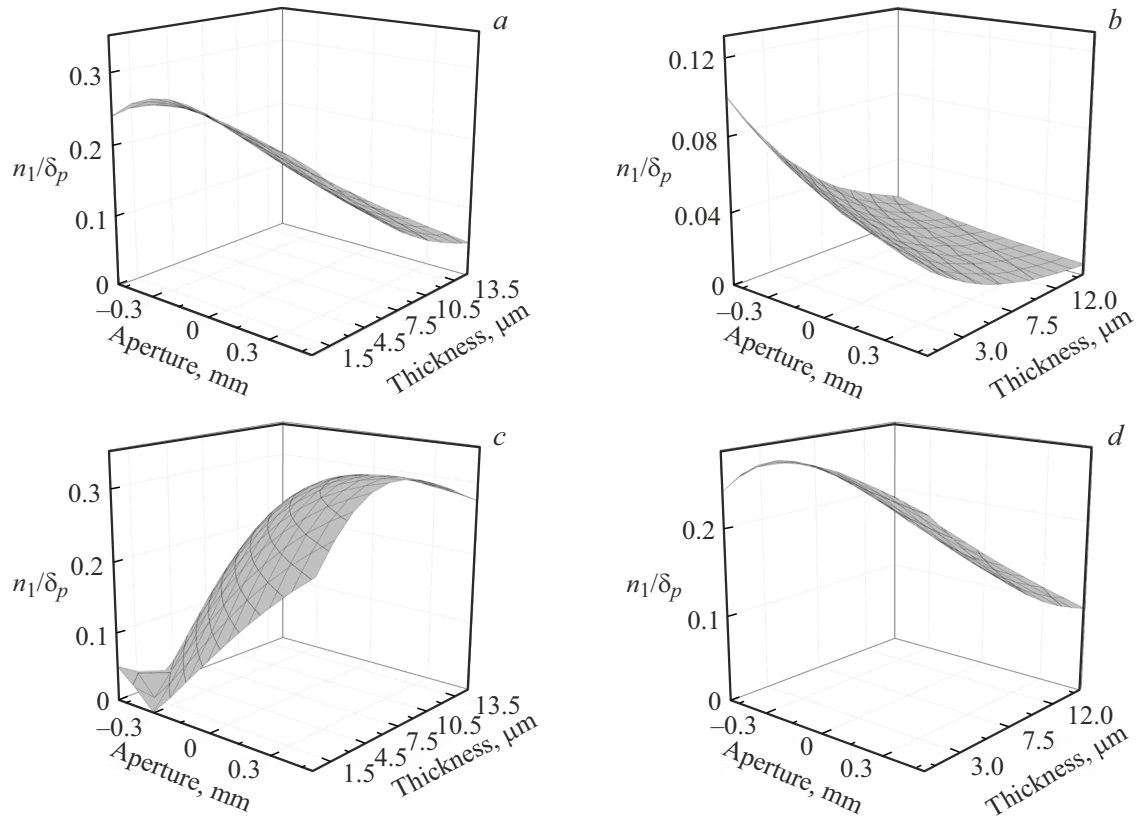

Figure 5. Two-dimensional spatial profiles of the first harmonic of the refraction index in the linear recording mode for two gratings on the first (a, b) and second layers (c, d).

inhomogeneity of grating profiles in the process of their holographic formation. The linear mode is the preferable way to obtain diffraction structures with better diffraction characteristics, since not only an increase in diffraction efficiency, but also the suppression of local minima in angular selectivity are to be expected in this mode.

Conclusion

The first generalized analytical model characterizing the process of formation of multiplexed chirped MIHDSs in PPM-LC with account for PIA and the recording mode under non-zero initial conditions for each diffraction layer and each diffraction structure was presented. The following patterns were identified via numerical modeling.

(1) In the nonlinear recording mode, the spatial profile is unique on each diffraction layer and for each sequentially formed structure and may transform in the process of recording. This is attributable to the fact that the monomer does not have enough time to diffuse into light areas and polymerizes quickly. The PIA process itself also contributes to this: the material is bleached in the course of formation, which also induces changes in the recording conditions.

(2) In the linear recording mode, the refraction index profiles for each layer and each grating also differ, but do not reveal any signs of transformation over time. In addition, the profile for each subsequent formed grating in the first layer may change from decreasing to increasing, which is associated with bleaching of the material during exposure and the variation of recording conditions over depth of the layer.

(3) Two-dimensional spatial profiles of the refraction index have two-dimensional inhomogeneity in linear and nonlinear recording modes and may differ not only from layer to layer, but also from one grating number to another. The inhomogeneity over layer width is induced in this case by the influence of phase inhomogeneity of recording radiation on the process of forming a diffraction structure, which has a period varying over layer width.

(4) To achieve high diffraction efficiency of multiplexed chirped MIHDSs, one needs to use the linear recording mode, since the level of inhomogeneity of the grating profiles is insignificant in this case.

Funding

This study was performed as part of the „Priority 2030“ academic leadership program.

Conflict of interest

The authors declare that they have no conflict of interest.

References

[1] V.G. Chigrinov, V.M. Kozenkov, H-S. Kwok. *Photoalignment of Liquid Crystalline Materials: Physics and Applications* (John Wiley & Sons, 2008). DOI: 10.1002/9780470751800

[2] V.G. Chigrinov. Crystals., **3** (4), 149–162 (2013). DOI: 10.3390/cryst3010149

[3] A. Komar, A. Tolstik, E. Melnikova, A. Muravsky. Applied Optics, **54** (16), 5130–5135 (2015). DOI: 10.1364/AO.54.005130

[4] E. Melnikova, A. Tolstik, I. Rushnova, O. Kabanova, A. Muravsky. Applied Optics, **55** (23), 6491–6495 (2016). DOI: 10.1364/AO.55.006491

[5] I. Rushnova, E. Melnikova, A. Tolstik, A. Muravsky. Optics Commun., **413**, 179–183 (2018). DOI: 10.1016/j.optcom.2017.12.029

[6] I.I. Rushnova, O.S. Kabanova, E.A. Melnikova, A.L. Tolstik. Nonlinear Phenomena in Complex Systems, **21** (3), 206–219 (2018).

[7] I.C. Khoo. *Liquid crystals* (John Wiley & Sons, 2022). DOI: 10.1002/9781119705819

[8] X. Yan, X. Wang, Y. Chen. Appl. Phys., **125**, 1–8 (2019). DOI: 10.1007/s00340-019-7173-4

[9] V.O. Dolgirev, S.N. Sharangovich. Bull. Russ. Acad. Sci. Phys., **86** (1), 18–23 (2022). DOI: 10.3103/S106287382201021X

[10] M.V. Shishova, A.Yu. Zherdev, D.S. Lushnikov, V.V. Markin, S.B. Odinokov. In *HOLOEXPO 2020: XVIII Mezhdunarodnaya konferentsiya po golografii i prikladnym opticheskim tekhnologiyam* (Mosk. Gos. Tekh. Univ., 2020), pp. 253–263 (in Russian).

[11] T. Wilm, J. Kibgies, R. Fiess, W. Stork. Photonics., **9** (6), 419 (2022). DOI: 10.1117/12.2596838

[12] E.A. Dovolnov, S.N. Sharangovich Proc. SPIE **6187**, Photon Management II, 454–460 (2006). DOI: 10.1117/12.673833

[13] H. Wang, B. Zhang, C. Han, J. Ding. Opt. Exp., **29** (20), 32377–32387 (2021). DOI: 10.1364/OE.440221

[14] D. Tosi. Sensors., **18** (7), 2147 (2018). DOI: 10.3390/s18072147

[15] C. Spiess, Q. Yang, X. Dong, V.G. Bucklew, W.H. Renninger. Optica, **8** (6), 861–869 (2021). DOI: 10.1364/OPTICA.419771

[16] D.I. Dudnik, I.A. Kvasova, K.O. Gusachenko, A.O. Semkin, S.N. Sharangovich. Izv. Vyssh. Uchebn. Zaved., Fiz., **61** (1), 51–58 (2018) (in Russian).

[17] E.A. Dovolnov, S.V. Ustyuzhanin, S.N. Sharangovich. Izv. Vyssh. Uchebn. Zaved., J., **49** (10), 1129–1138 (2006).

[18] A.O. Semkin, S.N. Sharangovich. Physics Procedia., **70**, 791–794 (2015). DOI: 10.1016/j.phpro.2015.08.269

[19] A.O. Semkin, S.N. Sharangovich. J. Phys.: Conf. Ser., **735**, 012030 (2016). DOI: 10.1088/1742-6596/735/1/012030

[20] D.I. Derevyanko, S.I. Aliev, E.F. Pen, V.V. Shelkovnikov. Optoelectron., Instrum. Data Process., **57** (6), 584–591 (2021). DOI: 10.3103/S8756699021060042

[21] F.K. Bruder, T. Fäcke, T. Rölle. Polymers., **9** (10), 472 (2017). DOI: 10.3390/polym9100472

Translated by D.Safin